Title: Probing developmental patterns of intracortical myelination using gray/white matter contrast and associations with cognitive abilities and psychopathology in youth

Authors: Linn B. Norbom[a,b*], Nhat Trung Doan[a], Dag Alnæs[a], Tobias Kaufmann[a], Torgeir Moberget[a], Jarek Rokicki[a,b], Ole A. Andreassen[a], Lars T. Westlye[a,b], Christian K. Tamnes[b,c]

[a] Norwegian Centre for Mental Disorders Research (NORMENT), KG Jebsen Centre for Psychosis Research, Division of Mental Health and Addiction, Oslo University Hospital & Institute of Clinical Medicine, University of Oslo, Oslo, Norway

[b] Department of Psychology, University of Oslo, Norway

[c] Department of Psychiatry, Diakonhjemmet Hospital, Oslo, Norway

*Corresponding author P.O. box 1094 Blindern, 0317 Oslo, Norway.

l.c.b.norbom@psykologi.uio.no

Abstract

Background: Cortical myeloarchitecture shows substantial development across childhood and adolescence, and aberrations in these trajectories are relevant for a range of mental disorders. The differential myelination of the cortex can be approximated using signal intensities in T1-weighted magnetic resonance images (MRI). **Methods:** To test the sensitivity of grey/white matter contrast (GWC) to age and individual differences in psychopathology and general cognitive ability in youth (8-23 years), we formed data-driven psychopathology and cognitive components using a large population-based sample, the Philadelphia Neurodevelopmental Cohort (PNC) (n=6487, 52% females). We then tested for associations with regional GWC defined by an independent component analysis (ICA) in a subsample with available MRI data (n=1467, 53% females). **Results**: The analysis revealed a global GWC component, which showed an age-related decrease from late childhood and across adolescence. In addition, we found regional anatomically meaningful components with differential age associations explaining variance beyond the global component. When accounting for age and sex, both higher symptom levels of anxiety or prodromal psychosis and lower cognitive ability were associated with higher GWC in insula and cingulate cortices and with lower GWC in pre- and postcentral cortices. We also found several independent regional associations with anxiety, prodromal psychosis and cognitive ability. **Conclusion:** Independent modes of GWC variation are sensitive to global and regional brain developmental processes, possibly related to ongoing intracortical myelination, and individual differences in regional GWC are associated with both mental health and general cognitive functioning.

Keywords: adolescence; brain development; mental health; MRI; myelination; signal intensity

Introduction

Adolescence is a time of extensive changes in the sociocultural domain, as well as within body, cognition, emotion and behavior (1, 2). Brain development during this period involves multiple biological processes that dynamically interact with the environment, and shows temporal and spatial heterogeneity across tissue types, measures and individuals (3-6). Increased knowledge about these brain developmental patterns and their individual differences is key to inform ontogenetic models of psychopathology.

Although current psychiatric diagnostic tools rely on manifest symptoms that often appear relatively late in illness progression, numerous mental disorders are considered to have a neurodevelopmental origin (7, 8), with additional risk factors related to social behavior and adverse effects of drug (9) and alcohol use. Moreover, common symptoms of mental illness form spectra in the general population (10-13). Neuroimaging studies using population based youth samples may thus provide early identification of individuals at risk and insight into the development of mental disorders, and discern brain phenotypes associated with the full range of variation in symptoms of mental illness.

The information processing analogy of the brain has provided a useful framework for the study of brain aberrations in clinical populations (14). An underlying assumption is that a healthy brain is characterized by efficient communication between regions, made possible by a structural backbone of myelinated axons and pathways. Myelin is key for efficient neural signaling as it increases speed and reliability of the nerve signal, provides support and prevents aberrant sprouting of nerve connections (15, 16). Neuroimaging studies have described developmental trajectories (3, 17) and case-control differences (18) in the organization and microstructure of these white matter pathways. A recent finding in an overlapping sample, indicate that frontotemporal white matter dysconnectivity is a transdiagnostic brain phenotype, associated with both higher levels of psychopathology and lower cognitive abilities (19).

Importantly, beyond white matter, the cerebral cortex is also myelinated, and intracortical myelination is a crucial feature of brain development (20), of which maturational timing conforms with a general posterior-anterior gradient, with additional regional specificity as highly myelinated regions, such as sensorimotor and early association cortices, mature early (20, 21). Cortical myelin content, as assessed *in vivo* using magnetic resonance imaging (MRI), has been linked to cognitive performance in youth (22) and adults (23), and abnormal intracortical myelination is a candidate mechanism for common mental disorders (8, 16, 24, 25). Compared to closely related non-human primates, postnatal intracortical myelination in

humans is exceptionally extended (26). Although there are clear benefits to allow for prolonged environmental influences on brain circuit establishment and refinement, this human-specific shift in timing and extension of cortical development may come at a cost, as diverse forms of psychopathology typically emerge during adolescence (27).

Cholesterol in myelin is a major determinant of the intensity in the T1-weighted MRI signal (28, 29), and cortical grey matter intensity has been shown to correspond closely with histologically based myelin profiles (30), and specifically with myelin rather than iron content (31). The differential myelination of the cerebral cortex can be approximated using the grey/white matter contrast (GWC) of the T1-signal intensity. GWC exhibits significant heritability (32), shows regional aging related patterns (33), and has been found to predict age more accurately than cortical thickness (34). Although dysmyelination is a viable candidate mechanism for brain network dysfunction, few studies have examined this measure in relation to mental health, and only in adults with psychosis (35-37).

The present study aimed to test the sensitivity of GWC to individual differences in age and psychopathology in youth (8-23 years). We used the Philadelphia Neurodevelopmental Cohort (PNC, n=6487) to develop data-driven clinical and cognitive components (19). In a subsample with available MRI data (n=1467), we performed an independent component analysis (ICA) of vertex wise GWC across the brain surface and tested for associations with age, different psychopathology components, and general cognitive ability. We hypothesized that GWC generally would show a negative association with age, reflecting the protracted myelination of the cortex, but also would show regional age-related patterns. Next, we hypothesized that youth with increased symptoms of psychopathology or lower cognitive ability would show regionally higher GWC, indicating lower levels of intracortical myelin.

Methods and Materials

Participants

The analyses were based on the publicly available PNC (permission #8642), a large population based sample comprising MRI, cognitive, clinical and genetic data (38, 39). The institutional review boards of the University of Pennsylvania and the Children's Hospital of Philadelphia (CHP) approved all study procedures, and written informed consent, as well as parental permission for individuals under the age of 18 years, were obtained (40). CHP recruited participants through a previous separate study enrollment (41). More than 10,000 participants underwent psychiatric and cognitive assessment, and 1601 of these individuals

were randomly selected for neuroimaging after stratification by age and sex (42). Further details on the procedures and project are described elsewhere (38, 40, 41).

We formed data-driven cognitive and clinical components using a larger sample of 6487 individuals (male=3108, female=3379) aged 8-22 years (mean= 13.8 years, SD=3.7 years) from the PNC as reported previously (19), and then tested for associations with GWC in a subsample of individuals with available and quality controlled MRI data. From 1601 available scans, we excluded participants with severe medical health conditions (n=70), based on a severity index rating by trained personnel in the PNC study team (43), or due to incomplete or poor quality MRI data (n=64, see below). The final MRI sample consisted of 1467 individuals (776 females) aged 8.2-23.2 years (mean=15.1 years, SD=3.6 years). Of these, 66 and 65 participants had missing clinical and cognitive data, respectively, and were excluded from relevant analyses.

Clinical assessment and data-driven decomposition of psychopathology

The clinical assessment consisted of a computerized and modified version of the neuropsychiatric interview Kiddie-Schedule for Affective Disorders and Schizophrenia (K-SADS). This interview assesses psychological treatment history, and lifetime occurrence of psychopathology. For participants aged 11-17, information from collaterals were included, while this was the only source for 8-10 year old participants (38). Using the larger set of participants (n=6487), we submitted 129 clinical symptom score items, covering 18 clinical domains, to ICA using ICASSO (44), as reported previously (19). The analysis yielded seven psychopathology components. In addition, as a general measure of psychopathology, we computed the mean subject weight across these components.

Cognitive assessment and definition of a general cognitive factor

Participants completed a computerized test battery evaluating a range of cognitive domains, including executive control, episodic memory, complex cognition, social cognition and sensorimotor speed (41). To estimate general cognitive ability, we included performance scores from 17 diverse tests in a principal component analysis (PCA) in the larger set of participants (n=6487) as reported previously (19). All raw scores were age residualized by linear regression, and standardized before running the PCA. The first factor was extracted as a general measure of cognitive function (gF), explaining 12% of the variance.

MRI acquisition and processing

MRI scans were acquired on a single 3T Siemens TIM Trio whole-body scanner without any software or hardware upgrades (38) (see Supplemental Materials). We used FreeSurfer 5.3 (http://surfer.nmr.mgh.harvard.edu) for cortical reconstruction and volumetric segmentation, including removal of non-brain tissue, intensity normalization, and tissue classification (45-48). To assess the quality of the cortical reconstructions, we implemented a flagging procedure based on robust PCA for detecting signal to noise-, and segmentation outliers (49, 50). We carefully inspected flagged datasets, and minor edits were performed when necessary (n= 459). Scans from 63 participants were excluded due to poor image quality.

Based on previous implementations (35, 51, 52), for each participant, we sampled signal intensities from the non-uniform intensity normalized volume (nu.mgz) using the FreeSurfer function mri_vol2surf. For each vertex, grey matter intensities were sampled at six equally spaced points, starting from the grey/white boundary and ending 60% into cortical grey matter. We selected this endpoint to minimize contamination of voxels containing cerebrospinal fluid. White matter intensities were sampled at each vertex at 10 equally spaced points, starting from the grey/white boundary and ending at a fixed distance of 1.5 mm into subcortical white matter. To obtain single separate measures of grey- and white matter intensity per vertex, we calculated the average intensity value for each tissue type. GWC was then computed as: $100 * (\text{white} - \text{grey})/[(\text{white} + \text{grey})/2]$ (35), such that a higher value reflects greater difference between grey and white matter signal intensities. The GWC surface maps were then smoothed using a Gaussian kernel of 10 mm full width at half maximum (FWHM), for vertex wise analyses.

To compare the GWC measure with the complimentary method of T1/T2 ratio, we created a mean GWC surface map of all participants, which was then converted to gifti format and transformed into the Human Connectome Project (HCP, (53)) standard mesh of 164,000 vertices (54). Additionally, to rule out confounding effects induced when comparing maps from different samples, we also created both GWC and T1/T2 ratio (21, 55) mean surface maps from the same subjects in two independent samples: Cam-CAN, obtained from the CamCAN repository (available at http://www.mrc-cbu.cam.ac.uk/datasets/camcan/) (56, 57), (male=10, female=8, age=18-29), and TOP (58, 59) (for MRI protocol, see Supplemental Materials), (male=10, female=10, age=15-54). Thus, allowing us to correlate maps obtained from the same subject using the two different methods. Specifically, we performed vertex wise Pearson correlations of our GWC mean map and the Conte69 mean T1/T2 myelin map provided by the HCP (55). We also performed vertex wise Pearson correlations of the GWC and T1/T2 ratio mean maps created from the independent datasets.

ICA-based decomposition of GWC across the surface

We performed ICA to decompose the GWC surfaces into spatially independent modes of variations using ICASSO (44). We used a model order of 15, pragmatically chosen based on a compromise between data reduction and total explained variance.

Statistical analyses

We first tested the strength and significance of the associations between each GWC IC and age. This was done by computing the T statistics of the linear and quadratic age effects of each GWC IC using General linear models (GLMs), covarying for sex, and p-values were corrected using the false discovery rate (FDR) correction procedure with a significance threshold of 0.05 (60). To visualize the observed effects we used locally weighted scatterplot smoothing (loess) and ggplot2 (61) visualization in R (https://www.r-project.org/).

Second, we tested for associations between the psychopathology component loadings and gF and GWC ICs using GLMs with age and sex as covariates. We also report associations with the quadratic age term when significant (removed from model when not significant). For each of the 15 GWC ICs, we ran GLMs where either one of the 7 psychopathology ICs, mean psychopathology score or gF was included in a separate model, as an independent variable, resulting in 135 (15*9) models in total. P-values were corrected using the FDR procedure with a significance threshold of 0.05 (60). To investigate possible interactions between age and psychopathology and gF on GWC ICs, we repeated the above models including an additional interaction term between these variables. To assess the dynamics of effects not necessarily well modeled by GLM we also performed a sliding window analysis and a subgroup visualization (see Supplemental Materials).

Third, to allow for comparison with a more conventional vertex wise approach, we examined the vertex wise effects of age, covarying for sex, and for psychopathology and gF, covarying for sex and age, on GWC, using GLM as implemented in the Permutation Analysis of Linear Models (PALM) toolbox (62). To assess statistical significance and account for multiple testing we used 10,000 permutations and family wise error (FWE) correction with threshold-free cluster enhancement (TFCE) (63) and a significance threshold of $p<0.05$, corrected.

Results

ICA decomposition of GWC

Figure 1 shows the 15 GWC components from ICASSO. In total, these components explained 29% of the total variance. With some notable exceptions, the maps were highly bilateral and symmetrical, and were region specific, except for a single global component. Regional specification corresponded well with regions separated within MRI based myelin maps and histological profiles, both concerning myelin content and developmental patterns (20, 21, 30).

Associations between GWC and age

The global GWC component showed a marked negative linear age association (t = -14.68, p= 1.27e-45) (Figure 1). Importantly, all remaining GWC ICs must be understood as reflecting independent variance beyond this global component. Components reflecting pre- and postcentral cortices showed strong linear negative age-associations (t=-24.34, p=3.70e-110 and t =-21.37, p=1.92e-88 respectively), and the occipital component also showed a highly significant negative association (t=-8.8, p=3.83e-18). The remaining ICs showed either slight or marked linear positive age associations with t-values ranging from 6.49 to 24.91 (all p< 0.05). The superior parietal and left lateral anterior components did not show a significant linear age effect. Loess visualization of the age associations on GWC ICs are shown in Figure 1.

Associations between GWC and psychopathology and gF

Figure 2 shows the results from the GLMs testing for associations with cognitive and clinical scores. There were several significant associations between GWC and anxiety (IC2) and prodromal psychosis (IC4). Specifically, higher loading on either anxiety or prodromal psychosis was both associated with higher GWC in left lateral posterior (t=3.01, p=1.78e-02 and t=2.85, p=2.60e-02, respectively) and insula and cingulate cortices (t=4.55, p=1.33e-04 and t=3.8, p=2.28e-03, respectively), and with lower contrast in pre- (t=-3.51, p=4.86e-03 and t=3.68, p=2.75e-03, respectively) and postcentral cortices (t=-3.28, p=8.91e-03 and t=-2.58, p=4.96e-02, respectively). Anxiety showed additional positive associations in prefrontal (t= 3.47, p=5.27e-03) and right lateral posterior cortices (t=3.00, p=1.78e-02). Prodromal psychosis showed an additional positive association in the visual cortex (t=4.38, p=2.45e-04), and additional negative associations in medial temporal (t=-3.03, p=1.78e-02) and superior frontal cortices (t=-3.16, p=1.29e-02).

Except for a single positive association between norm violating behavior and GWC in insula and cingulate cortices (t=3.05, p=1.76e-02), we found no significant associations between the other psychopathology components and GWC. There were, however, significant

associations between mean psychopathology score and several GWC components, but these overlapped with the effects of anxiety and/or prodromal psychosis.

General cognitive abilities, as indexed by gF, was positively associated with GWC in medial temporal (t=6.70, p=2.09e-09), pre- (t=4.12, p=6.70e-04) and postcentral (t=2.78, p=3.07e-02), and orbitofrontal cortices (t=6.83, p=1.76e-09), and negatively associated with GWC in insula and cingulate (t=-6.49, p= 5.48e-09), superior parietal (t=-2.92, p=2.19e-02), right lateral posterior (t=-2.77, p=3.07e-02), and visual cortices (t=-4.60, p=1.25e-04). Six of these eight associations between general cognitive ability and GWC spatially overlapped with associations between psychopathology and GWC, but with effects in the opposite direction. The correlation with gF loading was -0.14 and -0.13 for anxiety and prodromal psychosis loading respectively.

We found no significant interactions between age and psychopathology or gF on the GWC ICs. For GLMs with interaction term, sliding window results, and loess subgroup visualization, we refer to the Supplemental Material (Supplementary Figures 1-3).

Vertex wise associations between GWC and age, psychopathology and gF

Figure 3 shows the results from the conventional vertex wise analyses. Briefly, permutation testing revealed a near global negative association between age and GWC, indicating decreasing GWC in widespread regions with increasing age. Strongest negative associations were seen in regions around the central sulcus (Supplementary Table 1). These results generally correspond well with the results from the ICA approach. Results on vertex wise associations between psychopathology and gF and GWC are reported in the Supplemental Material (Supplementary Figure 4). Briefly, there were no significant associations of the psychopathology components, but negative significant associations with gF and GWC.

Comparison between GWC map and T1/T2 ratio myelin map

Figure 4 depicts the mean GWC surface map from all participants compared to the Conte69 mean T1/T2 ratio myelin map provided by HCP. Highly myelinated cortical regions within the myelin map, such as sensorimotor and early association regions, showed low GWC, while regions such as the prefrontal and premotor cortex, where myelination is low, showed high GWC. The vertex wise correlation between the two maps was 0.58. Using two independent datasets with both GWC and T1/T2 ratio maps from the same individuals, we found vertex wise correlations of -0.54 and -0.77, respectively.

Discussion

Cortical myeloarchitecture develops across childhood and adolescence, and based on the current study individual differences in intracortical myelination likely has clinical relevance for a range of mental disorders, in particular anxiety and psychotic disorders. Based on conventional T1-weighted brain scans from 1467 children and adolescents, we approximated intracortical myelination using the contrast in signal intensity between the cortex and subjacent white matter across the brain, where we show substantial similarities with myelin maps estimated using T1/T2 ratios. We found a global blurring of the GWC with increasing age, possibly reflecting protracted intracortical myelination across the brain surface, with additional regional developmental patterns. Across individuals, regional GWC was associated with symptom burden, with significant associations to symptoms of anxiety and prodromal psychosis, and with general cognitive ability.

A broad range of psychopathology components were identified using a data-driven approach and regional GWC was found to be associated with symptom levels of psychopathology within components reflecting several forms of anxiety and a component reflecting positive prodromal and advert psychosis. Higher levels of either anxiety or prodromal psychosis were associated with higher GWC in left lateral posterior and insula and cingulate cortices, and lower contrast in sensorimotor cortices. Anxiety also showed positive associations in prefrontal and right lateral posterior cortices, while prodromal psychosis showed a positive association in the visual cortex and negative associations in medial temporal and superior frontal cortices. Although our original hypothesis was that increased symptom burden would be linked to regionally higher GWC (reflecting less intracortical myelination), intracortical aberrations in both directions have been reported in prior studies (see below).

There is accumulating evidence for abnormal intracortical myelination as a potential mechanism for brain network dysfunction in neurodevelopemental disorders, and a potential causal process of psychosis in particular (16). Myelin-related abnormalities in psychosis is indicated by genetic association studies (64), post mortem studies (65, 66) and from the notion that psychotropic treatments have effects on myelin, and its plasticity and repair, that may substantially contribute to their effects (67). Two previous studies have investigated GWC in adults with schizophrenia with similar methods to the current study. Kong et al. (36) reported decreased GWC in frontal and temporal regions, while Jørgensen et al. (35) in a larger study reported the opposite i.e. increased GWC, yet in separate sensorimotor regions. Somewhat inconsistent with these studies, our results indicate that higher psychosis symptom

levels in adolescents are associated with decreased GWC in pre- and postcentral cortices extending into superior frontal cortex and with increased GWC in left lateral posterior, insula and cingulate, and visual cortices. The discrepancy could be due to analysis approach, sample age, or clinical characteristics. GWC studies on ultra-high risk samples and first episode psychosis would be a good intermediate to better understand our findings in the context of the psychosis spectrum. In addition to associations with prodromal psychosis, we also found associations with anxiety in partly overlapping regions.

We also investigated associations between general cognitive ability and GWC, hypothesizing that higher cognitive ability would be associated with lower GWC. The results indeed showed negative correlation in insula and cingulate, superior parietal, right lateral posterior, and visual cortices, but also positive associations in medial temporal, pre- and postcentral, and orbitofrontal cortices. Interestingly, most of these regions overlapped with regions in which we found associations between GWC and psychopathology, with effects consistently in the opposite direction.

A few prior studies measuring either GWC or T1/T2 ratio have reported associations with cognitive functioning (22, 23, 68). For example, a study on youth reported that brain age gap computed using GWC was strongly related to IQ (22). The effects in this study were driven by “decreased age” in sensorimotor regions and “increased age” in association cortices. Correspondingly, we found higher GWC in sensorimotor regions for participants with high cognitive functioning, and lower GWC in large posterior regions, particularly in the right hemisphere. The observation that several of the GWC regions associated in gF overlapped with regions associated with psychopathology, correspond well with a separate study, also on the PNC sample, which reported that gF and the mean psychopathology score share genetic contribution (19).

The global GWC component showed an age-related decrease across late childhood and adolescence. This fits well with prior studies employing both MRI-based cortical intensity measures and post mortem histology. For instance, a study investigating cortical signal intensity reported a steady decrease from childhood to adulthood (51), while a study employing T1/T2 ratio reported an ongoing intracortical myelination process from 8 years of age extending well into adulthood (68). Correspondingly, a post mortem study reported that the maturation of human intracortical myelination extends past late adolescence (26).

Beyond the global age-related decrease in GWC, regional components showed both positive and negative age effects, which may be understood as regionally protracted and accelerated development, respectively. For instance, components encompassing primary

sensorimotor or occipital regions showed negative associations with age. These regions have a high myelin content and mature early (20, 21). In comparison, e.g. the frontal lobe and temporal pole are known to continue intracortical myelination into the third and fifth decade of life respectively (68, 69), and the frontal lobe shows peak gray matter signal intensity later than the age range of the current sample (51). Correspondingly, components capturing these regions in the present study showed positive age associations, which together with the global negative age effect may indicate regionally protracted development.

Our GWC map showed high consistency with a mean T1/T2 cortical myelin map provided by HCP (21). The pattern of differentially myelinated cortical regions within the myelin map was captured by corresponding regional differences in GWC. The moderate correlation between the two maps could partly reflect differences in age range, as well as scanner related properties. This was partly supported by a similar and stronger vertex wise correlation observed between the mean GWC and T1/T2 ratio maps created from the same subjects using two smaller in-house datasets. Still, the strength of the correlations indicates that although the measures share variance, they may also have specific, unique properties.

Although our GWC map corresponded well with established notions of intracortical myelin (20, 21), some important limitations should be noted. Importantly, GWC is a measure that also includes white matter intensity, while the T1/T2 ratio exclusively measures cortical properties. We can only speculate whether regional and individual differences in GWC maps are driven by differences in signal intensity in cortical grey matter, white matter or more likely a combination of the two. It is also an indirect measure of myelin content, as the intensity in T1-weighted images also reflect other biological properties, such as water content, iron, and dendrite density (37, 70, 71). Another limitation with the current study is the cross sectional design, which is a non-optimal indirect way of studying development (72).

The relevance of the current study is twofold. First, studies of individuals at risk for mental disorders have typically used genetic risk from family history, or clinical risk measured as symptoms in help seeking individuals (42). In contrast, the PNC sampling strategy taps into the continuum of psychopathology in youth. Thus, our findings may help define markers of neural dysfunction at both an earlier age and stage of psychopathology development. This is critical for identifying biomarkers useful for early detection, and eventually for prevention and early intervention (42, 73). The finding that aberrations are already present in generally healthy youth with increased levels of anxiety and prodromal psychosis is an important addition to the literature. Second, we used data-driven approaches to identify both a broad range of psychopathology components and regional patterns in GWC,

aiming to improve sensitivity and specificity, as associations between brain structure and psychopathology are typically small or moderate (see e.g. (50)).

To conclude, the results of the current study reveal that GWC globally decreases across late childhood and adolescence, likely partly reflecting the extended maturation of intracortical myelination. We additionally found regional developmental patterns possibly reflecting accelerated and protracted myelination. Across individuals, regional GWC was associated with symptom burden of anxiety and prodromal psychosis and general cognitive ability, supporting the clinical and neurocognitive relevance of this tissue contrast measure.

Acknowledgments and disclosures: This work was supported by the Department of Psychology, University of Oslo (LBN and CKT), the Research Council of Norway (#223273, #249795, FRIMEDBIO #230345 to CKT), the South-Eastern Norway Regional Health Authority (#2014097, 2016083), and the European Commission's 7th Framework Programme (#602450, IMAGEMEND). The Philadelphia Neurodevelopment Cohort is a publicly available dataset. Support for the collection of this dataset was provided by grant RC2MH089983 awarded to Raquel Gur, MD, PhD, and RC2MH089924 awarded to Hakon Hakonarson, MD, PhD. The participants were recruited through the Center for Applied Genomics at The Children's Hospital in Philadelphia. Data for this article was in part collected and shared by the Cambridge Centre for Ageing and Neuroscience (CamCAN). CamCAN funding was provided by the UK Biotechnology and Biological Sciences Research Council (grant number BB/H008217/1), with support from the UK Medical Research Council and University of Cambridge, UK. Data were also in part provided by the Human Connectome Project, WU-Minn Consortium (Principal Investigators: David Van Essen and Kamil Ugurbil; 1U54MH091657) funded by the 16 NIH Institutes and Centers that support the NIH Blueprint for Neuroscience Research; and by the McDonnell Center for Systems Neuroscience at Washington University. Parts of the data in the present paper have previously been presented as a poster at the Society for Neuroscience 2017 annual meeting, and a preprint is published on bioRxiv.org.

The authors report no biomedical financial interests or potential conflicts of interest.

References

1. Blakemore, S.J. and K.L. Mills, *Is adolescence a sensitive period for sociocultural processing?* Annu Rev Psychol, 2014. **65**: p. 187-207.
2. Crone, E.A. and R.E. Dahl, *Understanding adolescence as a period of social-affective engagement and goal flexibility.* Nat Rev Neurosci, 2012. **13**(9): p. 636-50.
3. Lebel, C. and C. Beaulieu, *Longitudinal development of human brain wiring continues from childhood into adulthood.* J Neurosci, 2011. **31**(30): p. 10937-47.
4. Tamnes, C.K., et al., *Development of the Cerebral Cortex across Adolescence: A Multisample Study of Inter-Related Longitudinal Changes in Cortical Volume, Surface Area, and Thickness.* J Neurosci, 2017. **37**(12): p. 3402-3412.
5. Herting, M.M., et al., *Development of subcortical volumes across adolescence in males and females: A multisample study of longitudinal changes.* Neuroimage, 2018. **172**: p. 194-205.
6. Whitaker, K.J., et al., *Adolescence is associated with genomically patterned consolidation of the hubs of the human brain connectome.* Proc Natl Acad Sci U S A, 2016. **113**(32): p. 9105-10.
7. Insel, T.R. and P.S. Wang, *Rethinking mental illness.* JAMA, 2010. **303**(19): p. 1970-1971.
8. Insel, T.R., *Rethinking schizophrenia.* Nature, 2010. **468**(7321): p. 187-193.
9. Murray, R.M., et al., *30 Years on: How the Neurodevelopmental Hypothesis of Schizophrenia Morphed into the Developmental Risk Factor Model of Psychosis.* Schizophr Bull, 2017.
10. van Os, J., et al., *A systematic review and meta-analysis of the psychosis continuum: evidence for a psychosis proneness-persistence-impairment model of psychotic disorder.* Psychol Med, 2009. **39**(2): p. 179-95.
11. Lubke, G.H., et al., *Maternal Ratings of Attention Problems in ADHD: Evidence for the Existence of a Continuum.* Journal of the American Academy of Child & Adolescent Psychiatry, 2009. **48**(11): p. 1085-1093.
12. Kelleher, I., et al., *Prevalence of psychotic symptoms in childhood and adolescence: a systematic review and meta-analysis of population-based studies.* Psychol Med, 2012. **42**(9): p. 1857-63.
13. Ferdinand, R.F., et al., *No distinctions between different types of anxiety symptoms in pre-adolescents from the general population.* J Anxiety Disord, 2006. **20**(2): p. 207-21.
14. Fornito, A. and E.T. Bullmore, *Connectomics: a new paradigm for understanding brain disease.* Eur Neuropsychopharmacol, 2015. **25**(5): p. 733-48.
15. Baumann, N. and D. Pham-Dinh, *Biology of oligodendrocyte and myelin in the mammalian central nervous system.* Physiol Rev, 2001. **81**(2): p. 871-927.
16. Bartzokis, G., *Neuroglialpharmacology: Myelination as a shared mechanism of action of psychotropic treatments.* Neuropharmacology, 2012. **62**(7): p. 2137-2153.
17. Krogsrud, S.K., et al., *Changes in white matter microstructure in the developing brain--A longitudinal diffusion tensor imaging study of children from 4 to 11years of age.* Neuroimage, 2016. **124**(Pt A): p. 473-486.
18. Thomason, M.E. and P.M. Thompson, *Diffusion Imaging, White Matter, and Psychopathology.* Annual Review of Clinical Psychology, 2011. **7**(1): p. 63-85.
19. Alnæs, D., et al., *Association of heritable cognitive ability and psychopathology with white matter properties in children and adolescents.* JAMA Psychiatry, 2018.
20. Deoni, S.C.L., et al., *Cortical maturation and myelination in healthy toddlers and young children.* NeuroImage, 2015. **115**(Supplement C): p. 147-161.

21. Glasser, M.F. and D.C. Van Essen, *Mapping human cortical areas in vivo based on myelin content as revealed by T1- and T2-weighted MRI.* J Neurosci, 2011. **31**(32): p. 11597-616.
22. Lewis, J.D., A.C. Evans, and J. Tohka, *T1 white/gray contrast as a predictor of chronological age, and an index of cognitive performance.* Neuroimage, 2018. **173**: p. 341-350.
23. Grydeland, H., et al., *Intracortical Posterior Cingulate Myelin Content Relates to Error Processing: Results from T1- and T2-Weighted MRI Myelin Mapping and Electrophysiology in Healthy Adults.* Cereb Cortex, 2016. **26**(6): p. 2402-10.
24. Davis, K.L., et al., *White matter changes in schizophrenia: evidence for myelin-related dysfunction.* Arch Gen Psychiatry, 2003. **60**(5): p. 443-56.
25. Lake, E.M.R., et al., *Altered intracortical myelin staining in the dorsolateral prefrontal cortex in severe mental illness.* Eur Arch Psychiatry Clin Neurosci, 2017. **267**(5): p. 369-376.
26. Miller, D.J., et al., *Prolonged myelination in human neocortical evolution.* Proceedings of the National Academy of Sciences, 2012. **109**(41): p. 16480-16485.
27. Paus, T., M. Keshavan, and J.N. Giedd, *Why do many psychiatric disorders emerge during adolescence?* Nat Rev Neurosci, 2008. **9**(12): p. 947-57.
28. Koenig, S.H., et al., *Relaxometry of brain: why white matter appears bright in MRI.* Magn Reson Med, 1990. **14**(3): p. 482-95.
29. Koenig, S.H., *Cholesterol of myelin is the determinant of gray-white contrast in MRI of brain.* Magn Reson Med, 1991. **20**(2): p. 285-91.
30. Eickhoff, S., et al., *High-resolution MRI reflects myeloarchitecture and cytoarchitecture of human cerebral cortex.* Hum Brain Mapp, 2005. **24**(3): p. 206-15.
31. Stuber, C., et al., *Myelin and iron concentration in the human brain: a quantitative study of MRI contrast.* Neuroimage, 2014. **93 Pt 1**: p. 95-106.
32. Panizzon, M.S., et al., *Genetic and environmental influences of white and gray matter signal contrast: a new phenotype for imaging genetics?* Neuroimage, 2012. **60**(3): p. 1686-95.
33. Vidal-Pineiro, D., et al., *Accelerated longitudinal gray/white matter contrast decline in aging in lightly myelinated cortical regions.* Hum Brain Mapp, 2016. **37**(10): p. 3669-84.
34. Salat, D.H., et al., *Age-associated alterations in cortical gray and white matter signal intensity and gray to white matter contrast.* Neuroimage, 2009. **48**(1): p. 21-8.
35. Jorgensen, K.N., et al., *Increased MRI-based cortical grey/white-matter contrast in sensory and motor regions in schizophrenia and bipolar disorder.* Psychol Med, 2016. **46**(9): p. 1971-85.
36. Kong, L., et al., *Comparison of grey matter volume and thickness for analysing cortical changes in chronic schizophrenia: a matter of surface area, grey/white matter intensity contrast, and curvature.* Psychiatry Res, 2015. **231**(2): p. 176-83.
37. Bansal, R., et al., *The effects of changing water content, relaxation times, and tissue contrast on tissue segmentation and measures of cortical anatomy in MR images.* Magn Reson Imaging, 2013. **31**(10): p. 1709-30.
38. Satterthwaite, T.D., et al., *Neuroimaging of the Philadelphia Neurodevelopmental Cohort.* NeuroImage, 2014. **86**: p. 544-553.
39. Satterthwaite, T.D., et al., *The Philadelphia Neurodevelopmental Cohort: A publicly available resource for the study of normal and abnormal brain development in youth.* Neuroimage, 2016. **124**(Pt B): p. 1115-9.

40. Calkins, M.E., et al., *The Philadelphia Neurodevelopmental Cohort: constructing a deep phenotyping collaborative.* Journal of child psychology and psychiatry, and allied disciplines, 2015. **56**(12): p. 1356-1369.
41. Gur, R.C., et al., *Age group and sex differences in performance on a computerized neurocognitive battery in children age 8-21.* Neuropsychology, 2012. **26**(2): p. 251-65.
42. Satterthwaite, T.D., et al., *Structural brain abnormalities in youth with psychosis spectrum symptoms.* JAMA Psychiatry, 2016. **73**(5): p. 515-524.
43. Merikangas, K.R., et al., *Comorbidity of Physical and Mental Disorders in the Neurodevelopmental Genomics Cohort Study.* Pediatrics, 2015. **135**(4): p. e927-e938.
44. Himberg, J., A. Hyvarinen, and F. Esposito, *Validating the independent components of neuroimaging time series via clustering and visualization.* Neuroimage, 2004. **22**(3): p. 1214-22.
45. Fischl, B., *FreeSurfer.* Neuroimage, 2012. **62**(2): p. 774-81.
46. Fischl, B., et al., *Whole brain segmentation: automated labeling of neuroanatomical structures in the human brain.* Neuron, 2002. **33**(3): p. 341-55.
47. Dale, A.M., B. Fischl, and M.I. Sereno, *Cortical surface-based analysis. I. Segmentation and surface reconstruction.* Neuroimage, 1999. **9**(2): p. 179-94.
48. Fischl, B., M.I. Sereno, and A.M. Dale, *Cortical surface-based analysis. II: Inflation, flattening, and a surface-based coordinate system.* Neuroimage, 1999. **9**(2): p. 195-207.
49. Hubert, M. and S. Engelen, *Robust PCA and classification in biosciences.* Bioinformatics, 2004. **20**(11): p. 1728-1736.
50. Moberget, T., et al., *Cerebellar volume and cerebellocerebral structural covariance in schizophrenia: a multisite mega-analysis of 983 patients and 1349 healthy controls.* Mol Psychiatry, 2017.
51. Westlye, L.T., et al., *Differentiating maturational and aging-related changes of the cerebral cortex by use of thickness and signal intensity.* NeuroImage, 2010. **52**(1): p. 172-185.
52. Westlye, L.T., et al., *Increased sensitivity to effects of normal aging and Alzheimer's disease on cortical thickness by adjustment for local variability in gray/white contrast: a multi-sample MRI study.* Neuroimage, 2009. **47**(4): p. 1545-57.
53. Van Essen, D.C., et al., *The Human Connectome Project: a data acquisition perspective.* Neuroimage, 2012. **62**(4): p. 2222-31.
54. Glasser, M.F., et al., *The minimal preprocessing pipelines for the Human Connectome Project.* NeuroImage, 2013. **80**: p. 105-124.
55. Van Essen, D.C., et al., *Parcellations and Hemispheric Asymmetries of Human Cerebral Cortex Analyzed on Surface-Based Atlases.* Cerebral Cortex, 2012. **22**(10): p. 2241-2262.
56. Taylor, J.R., et al., *The Cambridge Centre for Ageing and Neuroscience (Cam-CAN) data repository: Structural and functional MRI, MEG, and cognitive data from a cross-sectional adult lifespan sample.* Neuroimage, 2017. **144**(Pt B): p. 262-269.
57. Shafto, M.A., et al., *The Cambridge Centre for Ageing and Neuroscience (Cam-CAN) study protocol: a cross-sectional, lifespan, multidisciplinary examination of healthy cognitive ageing.* BMC Neurology, 2014. **14**(1): p. 204.
58. Kaufmann, T., et al., *Disintegration of Sensorimotor Brain Networks in Schizophrenia.* Schizophr Bull, 2015. **41**(6): p. 1326-35.
59. Skatun, K.C., et al., *Global brain connectivity alterations in patients with schizophrenia and bipolar spectrum disorders.* J Psychiatry Neurosci, 2016. **41**(5): p. 331-41.

60. Genovese, C.R., N.A. Lazar, and T. Nichols, *Thresholding of statistical maps in functional neuroimaging using the false discovery rate.* Neuroimage, 2002. **15**(4): p. 870-8.
61. Wickham, H., *ggplot2: Elegant Graphics for Data Analysis*. 2009: Springer-Verlag New York.
62. Winkler, A.M., et al., *Permutation inference for the general linear model.* Neuroimage, 2014. **92**: p. 381-97.
63. Smith, S.M. and T.E. Nichols, *Threshold-free cluster enhancement: addressing problems of smoothing, threshold dependence and localisation in cluster inference.* Neuroimage, 2009. **44**(1): p. 83-98.
64. Steen, V.M., et al., *Genetic evidence for a role of the SREBP transcription system and lipid biosynthesis in schizophrenia and antipsychotic treatment.* European Neuropsychopharmacology, 2017. **27**(6): p. 589-598.
65. Tkachev, D., et al., *Oligodendrocyte dysfunction in schizophrenia and bipolar disorder.* Lancet, 2003. **362**(9386): p. 798-805.
66. Uranova, N.A., et al., *Ultrastructural alterations of myelinated fibers and oligodendrocytes in the prefrontal cortex in schizophrenia: a postmortem morphometric study.* Schizophr Res Treatment, 2011. **2011**: p. 325789.
67. Bartzokis, G., *Neuroglialpharmacology: White matter pathophysiologies and psychiatric treatments*. Vol. 16. 2011. 2695-733.
68. Grydeland, H., et al., *Intracortical myelin links with performance variability across the human lifespan: results from T1- and T2-weighted MRI myelin mapping and diffusion tensor imaging.* J Neurosci, 2013. **33**(47): p. 18618-30.
69. Bartzokis, G., *Age-related myelin breakdown: a developmental model of cognitive decline and Alzheimer's disease.* Neurobiology of Aging, 2004. **25**(1): p. 5-18.
70. Righart, R., et al., *Cortical pathology in multiple sclerosis detected by the T1/T2-weighted ratio from routine magnetic resonance imaging.* Annals of Neurology, 2017. **82**(4): p. 519-529.
71. Bulk, M., et al., *Postmortem MRI and histology demonstrate differential iron accumulation and cortical myelin organization in early- and late-onset Alzheimer's disease.* Neurobiol Aging, 2018. **62**: p. 231-242.
72. Kraemer, H.C., et al., *How can we learn about developmental processes from cross-sectional studies, or can we?* Am J Psychiatry, 2000. **157**(2): p. 163-71.
73. Insel, T.R., *Translating scientific opportunity into public health impact: a strategic plan for research on mental illness.* Arch Gen Psychiatry, 2009. **66**(2): p. 128-33.

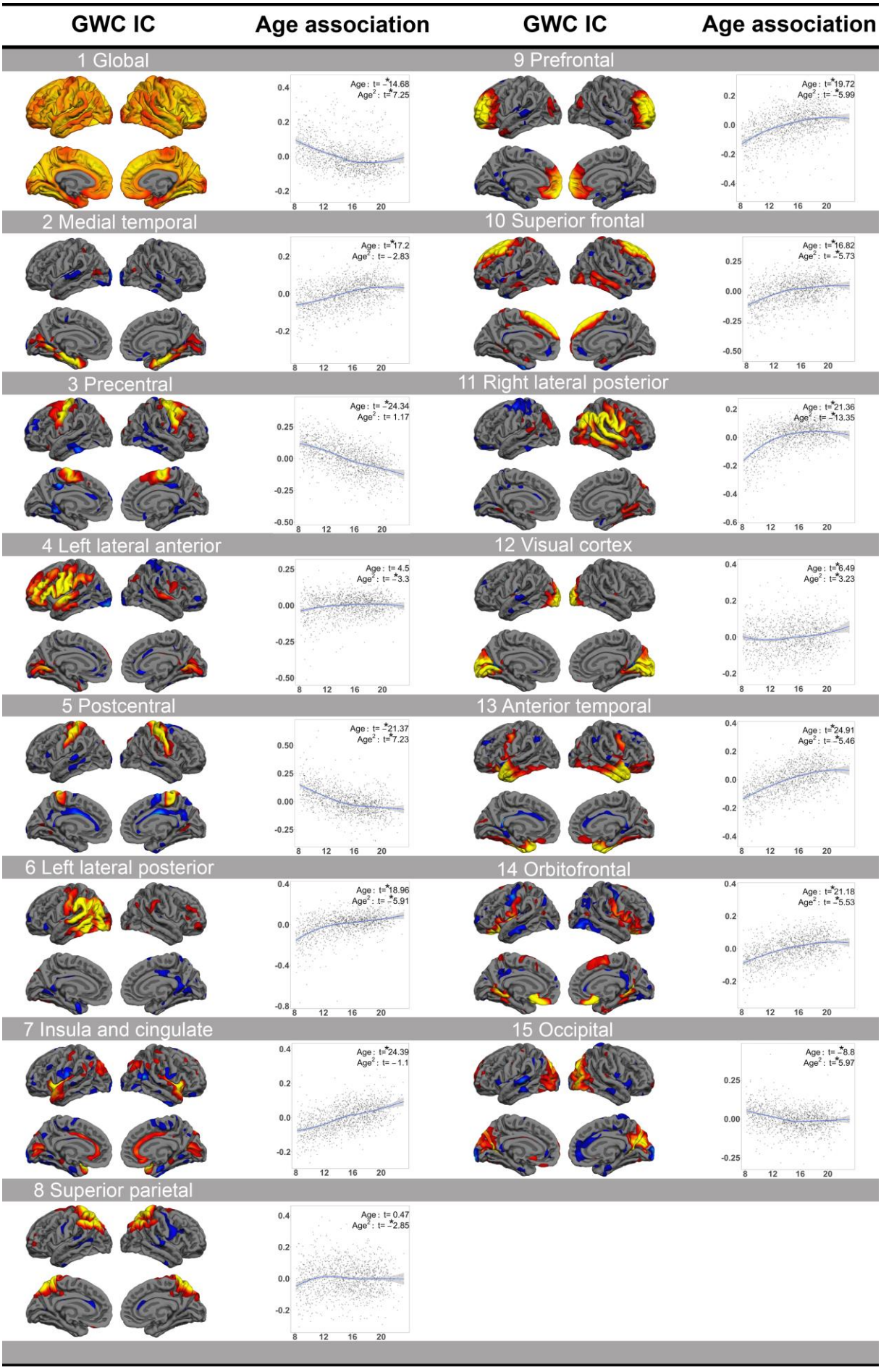

Figure 1. GWC independent components (ICs) and their associations with age. The GWC IC columns show the number, name and anatomical representation. GWC IC special maps are thresholded at 1-3 standard deviations (SDs), except "1 Global" which is thresholded at 1-9 SDs. The age association columns show a loess visualization of the age association depicted in blue with actual data points scattered. The t statistics for age and age^2, covarying for sex, are shown in the top right corners. * FDR corrected $p < 0.05$

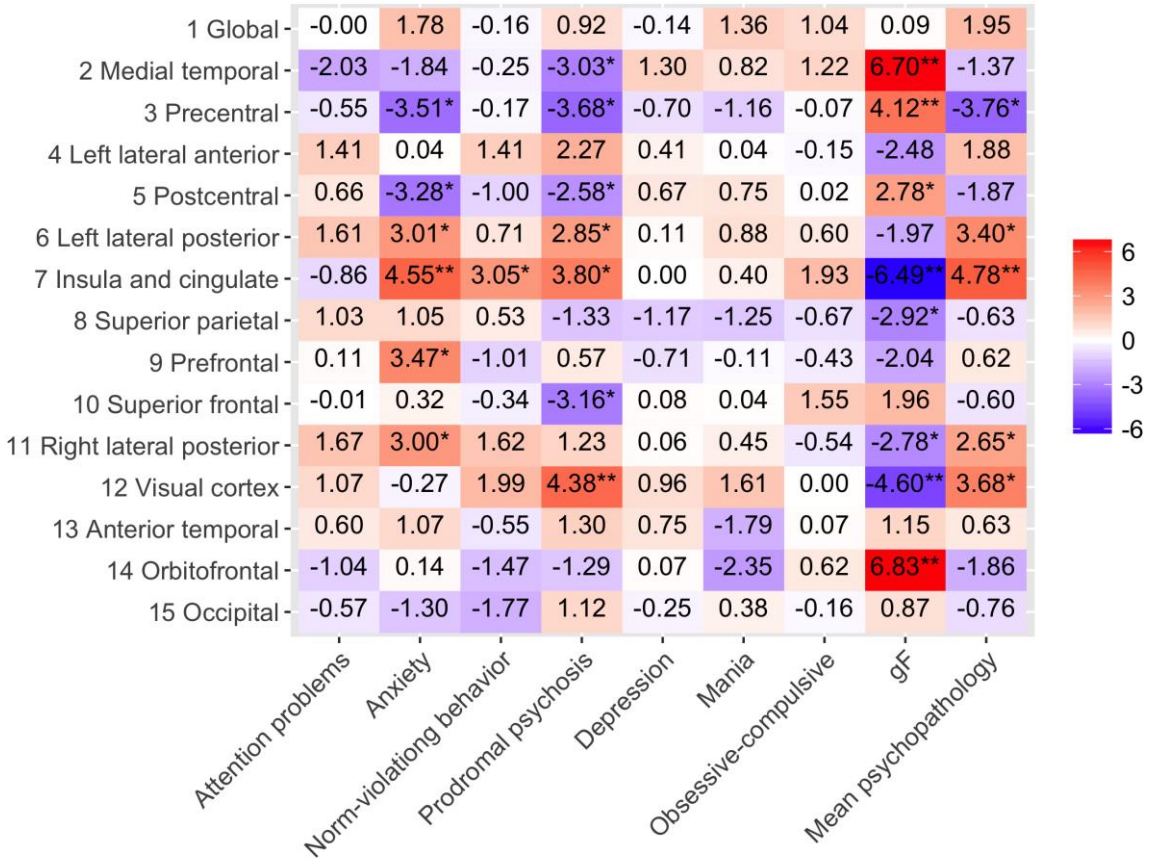

Figure 2. T statistics of the associations between GWC and psychopathology. The y-axis shows each GWC independent component (IC). The x-axis shows each psychopathology IC, gF, and mean psychopathology score. The map is color scaled so that red squares show positive associations, while blue squares show negative associations, covarying for age, age^2 when significant and sex. * corrected $p < 0.05$, ** corrected $p < 0.01$.

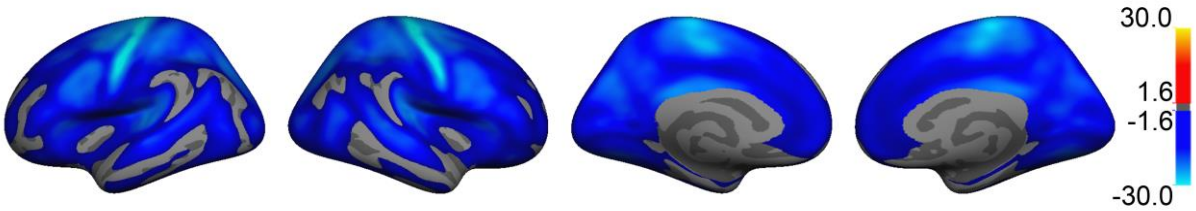

Figure 3. Vertex wise associations between age and GWC. T statistics are masked by FWE corrected p values thresholded at a minimum –log(p) of 1.6 to correct for two hemispheres. Blue regions represent a negative age association, while red regions would depict a positive association.

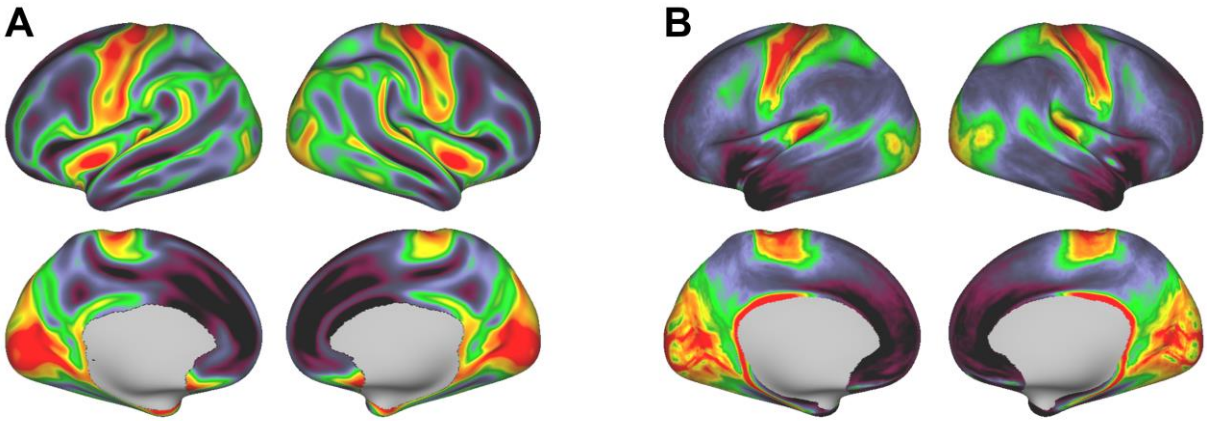

Figure 4. Mean GWC map vs T1/T2 myelin map. **A** depicts the mean GWC surface maps of the current sample. Warm colors represent regions with lower GWC, while cold colors represent regions with higher GWC. **B** depicts a mean T1/T2 myelin map from young adults, based on 69 subjects (male=38, female=31, age=9-45) (55). Warm colors are thought to represent regions with a high amount of intracortical myelin, while cold colors represent regions of low myelin content.

Supplemental information

Supplemental methods

MRI acquisition PNC

Signal excitation and reception was obtained using a quadrature body coil for transmit and a 32-channel head receiver coil. Gradient performance was 45mT/m, with a maximum slew rate of 200 T/m/s [1]. T1 weighted imaging was obtained using a magnetization prepared rapid-acquisition gradient-echo (MPRAGE) sequence (TR=1810 ms; TE=3.51 ms; FoV=180×240 mm; Resolution=0.94×0.94×1.0 mm). Receive coil (i.e. B1) shading was reduced by selecting the Siemens pre-scan normalize option, which corrects for B1 inhomogeneity based on a body coil reference scan [1].

MRI acquisition TOP

MRI scans were acquired on a single 3T GE 750 scanner. Signal excitation and reception was obtained using a 32-channel head receiver coil. T1 weighted imaging was obtained in the sagittal plane, with 1mm isotropic voxels and pulse sequence "Brain Volume imaging" (BRAVO). Flip Angle: 12, TI: 450, Receiver Bandwidth: 31.25, Freq: 256, Phase: 256, Freq DIR: S/I, NEX: 1.00, Phase FOV: 1.00.

Supplemental statistical analyses

Sliding window analysis

In order to investigate dynamics of possible effects not necessarily well modeled by standard linear models we performed a GLM sliding window width of 5 years and steps of 1 year, analyses. Here, GWC ICs were dependent variables, age and sex were covariates, and only psychopathology ICs or the gF component that had already shown a main effect, were chosen as separate independent variables. At each step, the t-statistics representing the association between relevant psychopathology ICs and gF on GWC ICs were extracted and standardized using Cohen's *d*. All p-values were FDR corrected with a significance threshold of 0.05 [2] for all windows.

Loess subgroup visualization

To visually assess the effects found by GLM and sliding window analyses we performed a subgroup visualization by loess ggplot in R. Here, only psychopathology ICs or the gF component that had already shown a main effect, were chosen as separate independent

variables. We fitted a curve on the full sample for the association between GWC ICs and age. We then identified participants with the lowest loading on relevant independent variables, and repeated the same spline fitting procedure on sub groups, after removing 50%, 80% and 90% of these participants respectively. Thus, beginning with the full sample and then continuously removing the "healthiest" (or for gF "lowest" performing) individuals, in order to inspect changes in the association. We chose the above-described four percentage groups after reviewing the spread of each relevant independent variable. Splines were then bootstrapped 1000 times in order to extract confidence intervals.

Supplemental results

Sliding window

Anxiety and prodromal psychosis showed positive age interactions with three separate GWC ICs, while gF showed one positive age interaction. Prodromal psychosis and gF additionally showed three separate negative age interactions (see Figure S2). In sum, although we did not find any significant GLM effects with an age interaction term, the sliding window approach still yielded trends toward age interaction effects for anxiety, prodromal psychosis and gF on several GWC ICs. As correction for multiple testing were solely performed across windows and not across the full set of tests, results should be interpreted with caution.

Loess subgroup visualization

For the loess subgroup visualization plots of anxiety, prodromal psychosis and gF, see Figure S2. In short, the visualization correspond well with clinical main effects reported from GLM analyses as well as the sliding window trends.

Vertex wise associations between anxiety, prodromal psychosis, gF and GWC

Permutation testing revealed no significant associations for either of the psychopathology ICs, but unthresholded t-statistic maps were in general in agreement with the effects revealed through ICA (Figure S4). There were vertex wise significant negative associations between gF and GWC in medial and posterior regions of the brain, consistent with the ICA results, albeit not capturing the positive effects.

Supplementary Tables

STRUCTURAL ROI	LH	RH
BANKS SUPERIOR TEMPORAL SULCUS	-9.71	-11.75
CAUDAL ANTERIOR CINGULATE	-8.15	-7.27
CAUDAL MIDDLE FRONTAL	-14.40	-13.56
CUNEUS	-11.23	-10.66
ENTORHINA	-0.72	-0.53
FUSIFORM	-6.43	-6.25
INFERIOR PARIETAL	-6.30	-7.57
INFERIOR TEMPORAL	-4.13	-2.53
ISTHMUS CINGULATE	-12.41	-11.84
LATERAL OCCIPITAL	-7.78	-8.94
LATERAL ORBITOFRONTAL	-5.11	-5.17
LINGUAL	-8.14	-8.68
MEDIAL ORBITOFRONTAL	-2.06	-2.19
MIDDLE TEMPORAL	-2.43	-2.01
PARAHIPPOCAMPAL	-0.61	-1.53
PARACENTRAL	-20.73	-20.20
PARSOPERCULARIS	-10.87	-11.56
PARSORBITALIS	-1.97	-5.75
PARSTRIANGULARIS	-9.60	-10.20
PERICALCARINE	-9.86	-9.87
POSTCENTRAL	-14.51	-14.51
POSTERIOR CINGULATE	-11.34	-11.11
PRECENTRAL	-19.59	-19.95
PRECUNEUS	-13.29	-12.85
ROSTRAL ANTERIOR CINGULATE	-3.74	-3.66
ROSTRAL MIDDLE FRONTAL	-4.81	-6.33
SUPERIOR FRONTAL	-9.44	-8.61
SUPERIOR PARIETAL	-13.95	-14.76
SUPERIOR TEMPORAL	-6.56	-6.07
SUPRAMARGINAL	-7.46	-9.22

FRONTAL POLE	-1.62	0.03
TEMPORAL POLE	0.67	2.72
TRANSVERSE TEMPORAL	-15.28	-15.85
INSULA	-5.47	-5.23

Table S1. ROI t statistic overview of age effects. The left column depicts names of each region of interest. The next two columns depict the mean t statistic in the left and right hemisphere respectively for the age effect, covarying for sex.

Supplementary Figures

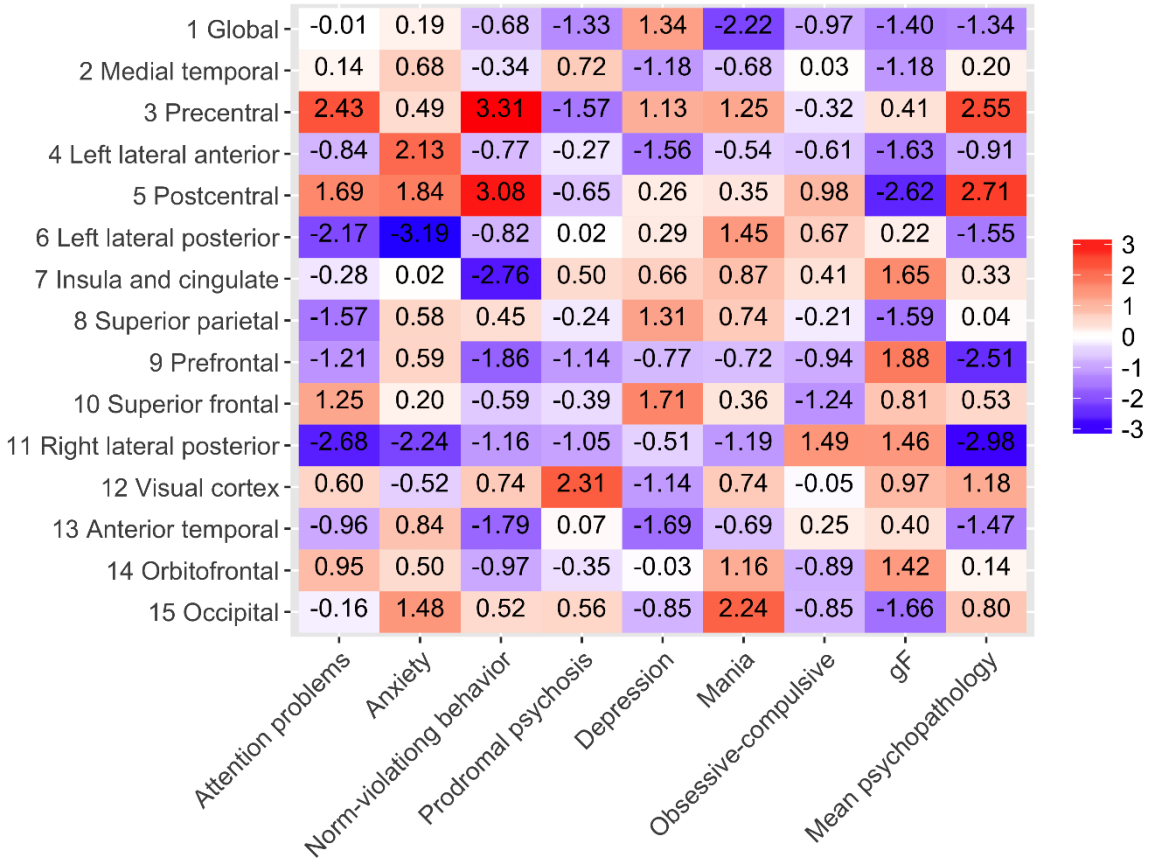

Figure S1. Interaction effects of psychopathology and age on GWC. The y-axis shows each GWC independent components (ICs). The x-axis shows each psychopathology IC, gF and mean psychopathology score. The map is color scaled so that red squares show positive associations, while blue squares show negative associations, covarying for age, age^2 when significant, and sex. * corrected $p < 0.05$, ** corrected $p < 0.01$.

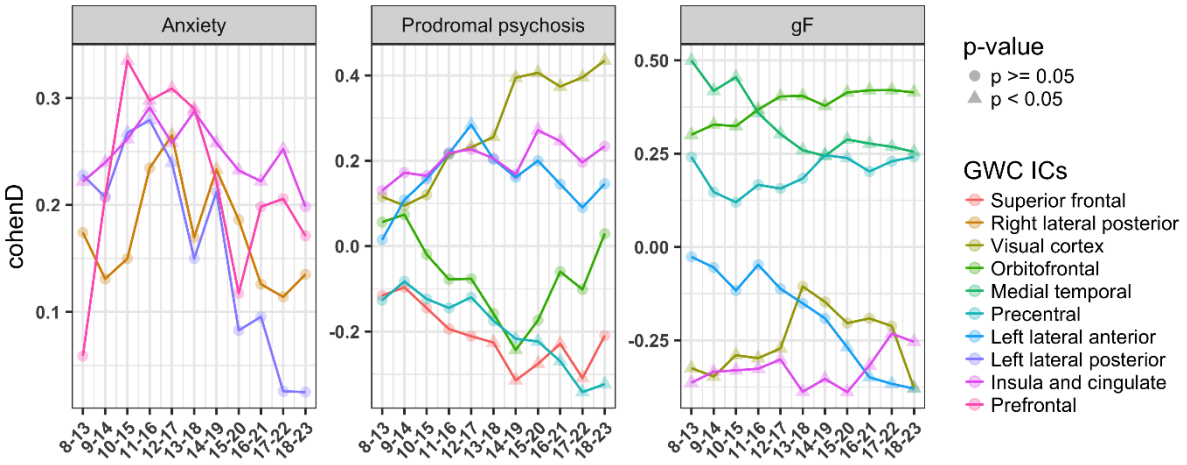

Figure S2. Sliding window width of 5 years and steps of 1 year analyses. GWC independent components (ICs) are depicted only if at least one significant age window was found. Left plot shows anxiety, middle plot shows prodromal psychosis and the right plot shows gF. The y-axis represent Cohen's D value of the strength of the associations, while the x-axis represents the age windows. Triangles on the line represent Cohen's D values with corrected $p < 0.05$.

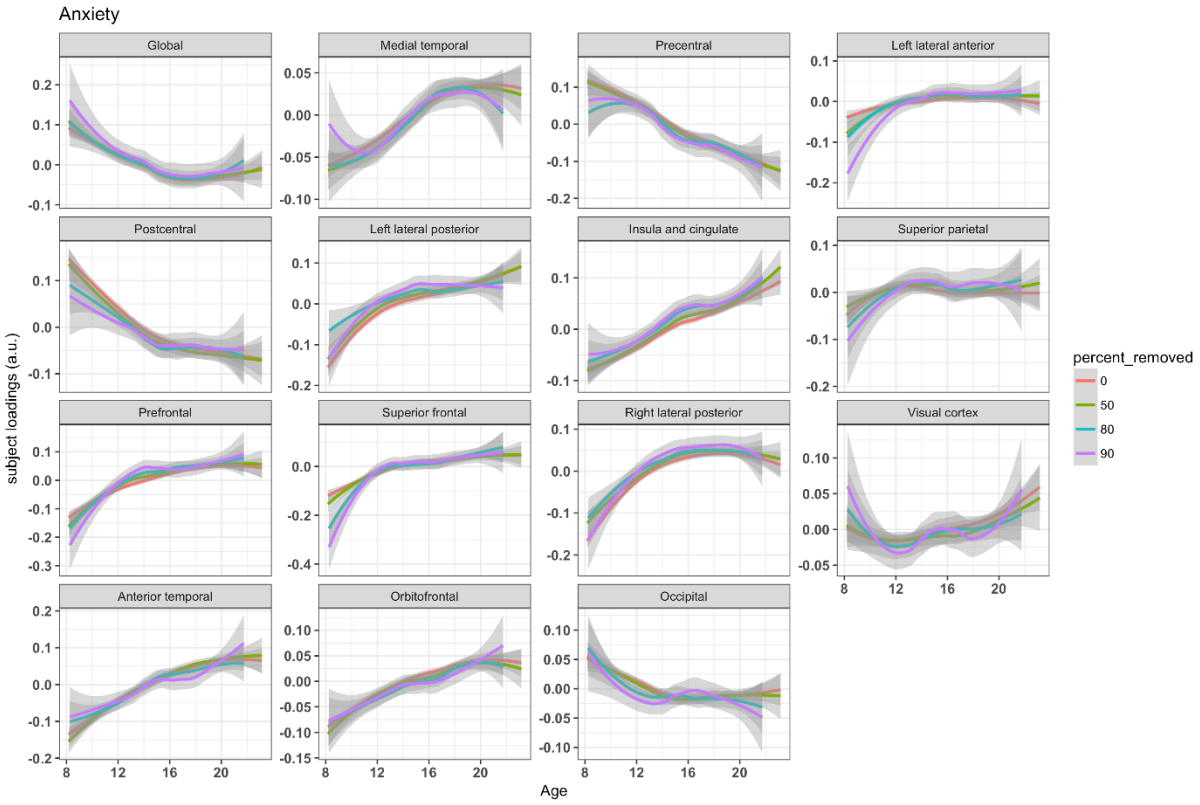

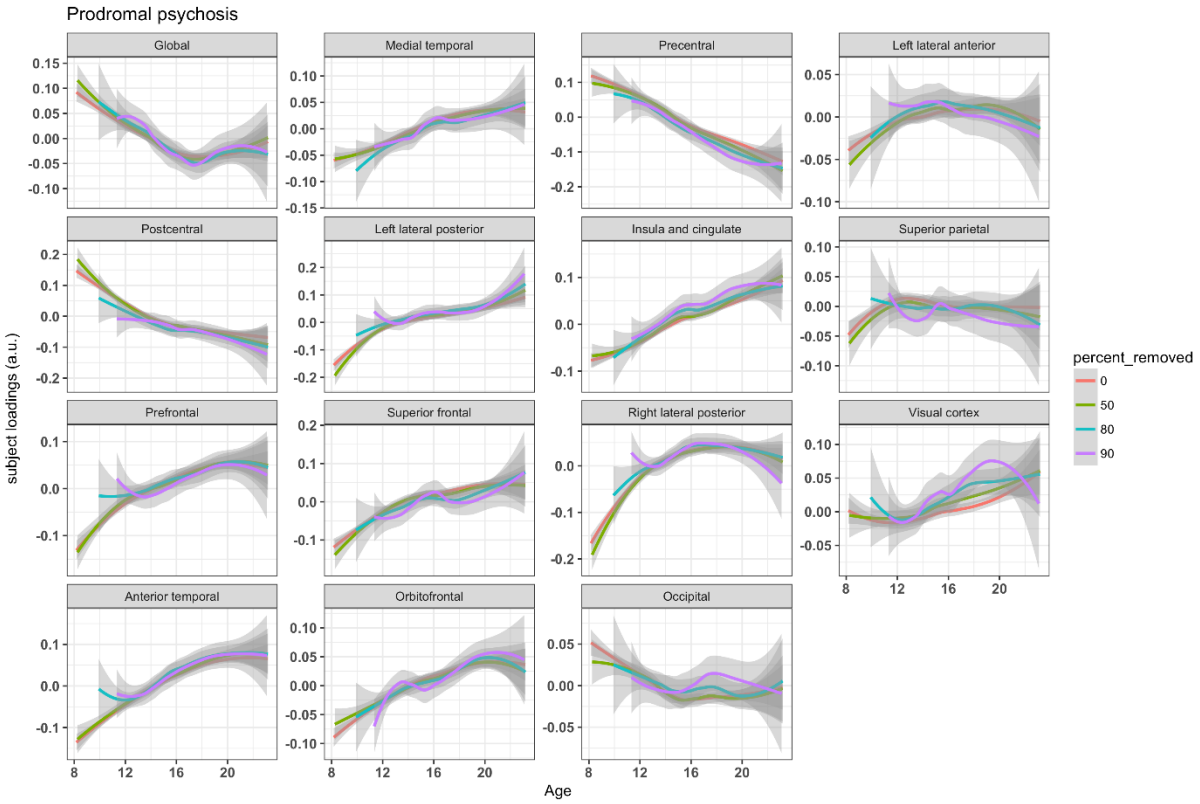

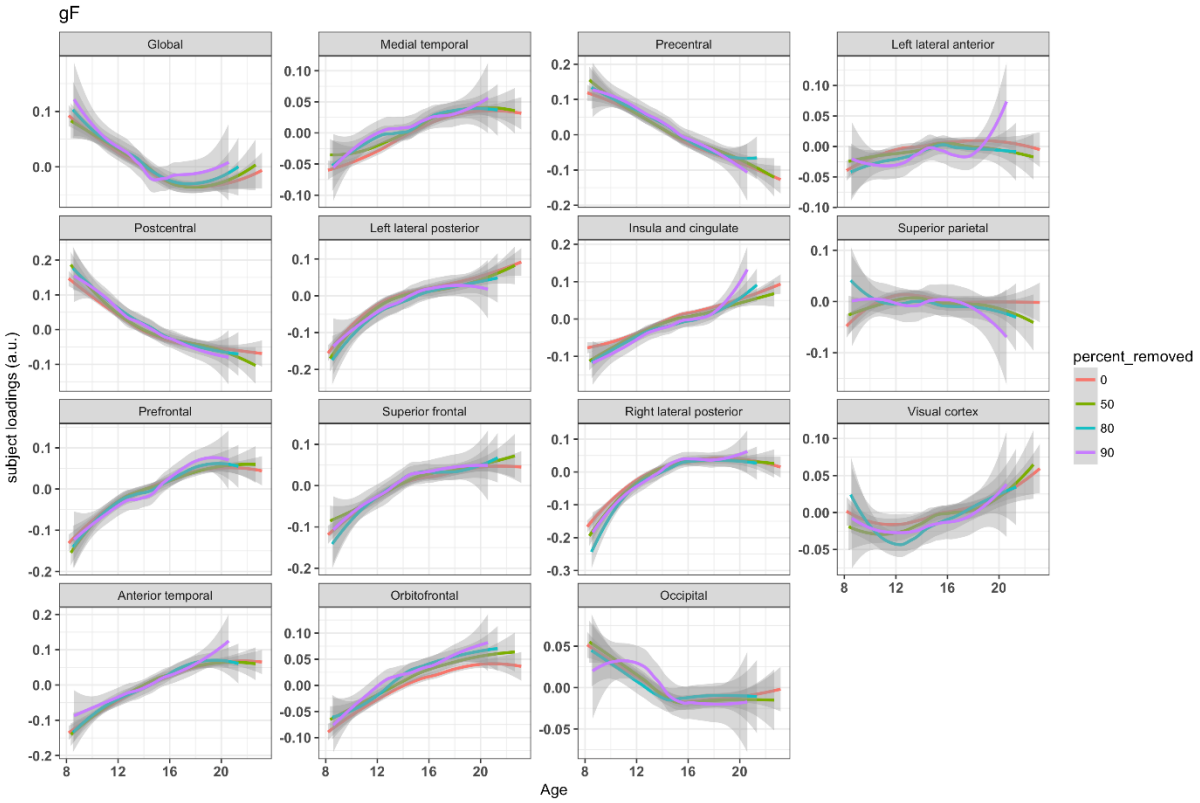

Figure S3. Loess subgroups visualization investigating the age-dynamic between psychopathology and GWC. The plots show the fitted curves for each GWC independent components (IC) for anxiety at the top, prodromal psychosis in the middle and gF at the bottom. The y-axes depicts the GWC IC loading, while the x-axis depicts age. The red line represents the full sample. The green, blue and purple line represents identical analyses after removal of individuals with the 50% 80% and 90% lowest psychopathology/gF loadings respectively. Shaded colored regions represent the confidence interval.

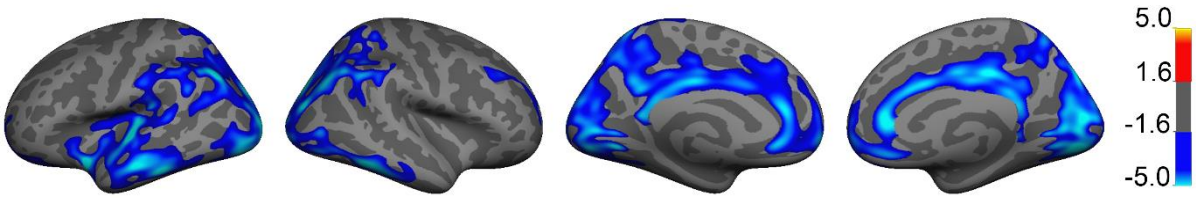

Figure S4. Vertex wise associations between gF and GWC. Permutation Analysis of Linear Models (PALM) on the associations of gF on GWC was performed. T statistics are masked by FWE corrected p values thresholded at a minimum –log(p) of 1.6 to correct for two hemispheres. Blue regions represent a negative gF association, while red regions would depict a positive association with gF.

Supplemental references

1. Satterthwaite, T.D., et al., *Neuroimaging of the Philadelphia Neurodevelopmental Cohort.* NeuroImage, 2014. **86**: p. 544-553.
2. Genovese, C.R., N.A. Lazar, and T. Nichols, *Thresholding of statistical maps in functional neuroimaging using the false discovery rate.* Neuroimage, 2002. **15**(4): p. 870-8.